agriculture

MDPI

Article

Friction and Wear Properties of Wheat Straw Powder Third Body on Steel-Steel Friction Pair

Chenglong Lian [1,2], Wei Zhao [3], Shumei Wang [1], Peng Zhang [4], Xiaoying Dong [1] and Yongfeng Li [1,*]

[1] Forestry College, State Forestry and Grassland Administration Key Laboratory of Silviculture in Downstream Areas of the Yellow River, Shandong Agricultural University, Taian 271018, China; lyjj917@sdau.edu.cn (C.L.); wsm@sdau.edu.cn (S.W.); xydong@sdau.edu.cn (X.D.)
[2] Postdoctoral Innovation Practice Base, Shandong Xiaguang Group Co., Ltd., Jining 277600, China
[3] Forestry College, Northwest Agricultural and Forestry University, Xianyang 712199, China; zhaoweixbnlkjdx@nwafu.edu.cn
[4] Nanjing Institute of Agricultural Mechanization, Ministry of Agriculture and Rural Affairs, Nanjing 210014, China; zhangpeng01@caas.cn
* Correspondence: lyf288@hotmail.com; Tel.: +86-538-8240610

Abstract: Third body plant fibers have an important influence on the friction and wear properties of metal friction pairs. In this study, wheat straw powder with different particle sizes was prepared, and a pin-on-disk friction tester was employed to evaluate the friction and wear properties of the wheat straw powder third body on steel friction pairs under various conditions. The results show that the straw powder played an isolation role in the steel–steel friction pair, which reduced the contact area between the pin and the disc and thus reduced the friction coefficient. Compared with the large particle size powder, the small particle size powder became embedded in the friction interface or in the groove caused by wear, buffered the friction stress, and reduced the friction coefficient and wear. When lubricants such as lubricating oil or lubricating grease were added, the friction coefficient was significantly reduced. Under the influence of lubricant, the particle size of straw powder had no significant effect on the wear. The results of this study can provide a reference for the third body friction and wear properties of straw powder and the design of friction pairs for metal parts.

Keywords: friction; wear; wheat straw powder; third body friction

Citation: Lian, C.; Zhao, W.; Wang, S.; Zhang, P.; Dong, X.; Li, Y. Friction and Wear Properties of Wheat Straw Powder Third Body on Steel-Steel Friction Pair. *Agriculture* **2022**, *12*, 882. https://doi.org/10.3390/agriculture12060882

Academic Editor: Francesco Marinello

Received: 17 May 2022
Accepted: 15 June 2022
Published: 18 June 2022

1. Introduction

About half of the world's energy is consumed in friction in various forms, and various forms of wear cause more than 80% of the damage of machine parts. Confirming the friction and wear properties of the parts is of great significance to the preservation and green development of various types of machinery [1]. The three-body abrasive wear caused by abrasive particles sandwiched between two contact surfaces has an important impact on the friction and wear of the surfaces [2,3]. The friction and wear properties of the third body depend on the material, hardness, particle size, and other parameters of the exogenous third body material [4,5]. When surface roughness is constant, the particle size and the external load affect the friction coefficient greatly [6]. When the ratio of particle size to surface roughness and the external load were the same, the friction coefficient increases with the decrease of surface roughness [7]. At relatively low loads, when the particle size is larger or the particle density is higher, the particle temperature might also be higher than the surface temperature, which induces an abnormal wear process [8]. The wear rate varies significantly with the size of the abrasive grains, and the wear rate can be predicted based on the size of the abrasive grains. Small-sized asperities are more prone to plastic deformation than large-sized asperities [9]. The particle size has a significant effect on the friction and wear properties of the particle. A large number of studies have shown that exogenous metals such as copper powder [10], copper–graphite powder [11], iron powder [12], and other powders have important effects on the friction and wear properties of friction pairs under various lubrication conditions [13–18]. Concurrently, in agricultural machinery research, many studies using three-dimensional scanning and other technologies are discovering that soil particles or other factors have an important influence on the wear and durability of the plowshare [19–21].

With the rapid development of the agricultural and forestry industry, agricultural and forestry machinery such as wheat harvesters are developing in large-scale, efficient and intelligent directions [22–24]. While such harvesters greatly improve efficiency, a large amount of wheat straw powder is produced during the working process. Some of it is collected or filtered by the purification device to avoid it impacting the operation of the equipment. However, some straw powder still enters the open friction pairs, such as connecting rods, worm gears, and racks and pinions inside the equipment, which has an impact on the friction and wear. However, whether these exogenous plant fiber powders entering the friction pairs are beneficial or harmful to the friction and wear properties of parts has not been verified.

In this study, the friction and wear properties of third body straw powder with different particle sizes on steel–steel friction pairs were investigated under the conditions of pure wheat straw powder, wheat straw powder mixed with lubricating oil, and wheat straw powder mixed with polytetrafluoroethylene (PTFE) grease. Combined with the observation of the worn surface with a microscope, the mechanism of exogenous straw powder on the friction and wear properties of the steel–steel friction pair was analyzed. Results of this study provide a basis for the theory and application of three-body friction and wear of plant fibers.

2. Materials and Methods

2.1. Wheat Straw Powder

The wheat straw of Shannong No. 27 was selected. After being ground by a pulverizer, it was sorted into 5 kinds with 20, 40, 60, 80, and 100 meshes. Fifty particles in each particle size sample were randomly selected, and the average particle size and aspect ratio were observed and measured by an optical microscope (SZX16, OLYMPUS). As shown in Figure 1, the corresponding average particle sizes and standard deviation are 0.90 mm ± 0.10 mm, 0.56 mm ± 0.07 mm, 0.43 mm ± 0.04 mm, 0.28 mm ± 0.02 mm, and 0.17 mm ± 0.01 mm, and the aspect ratios and standard deviation are 5.25 ± 1.27, 4.95 ± 1.05, 1.68 ± 0.68, 1.24 ± 0.17, and 1.18 ± 0.10, respectively.

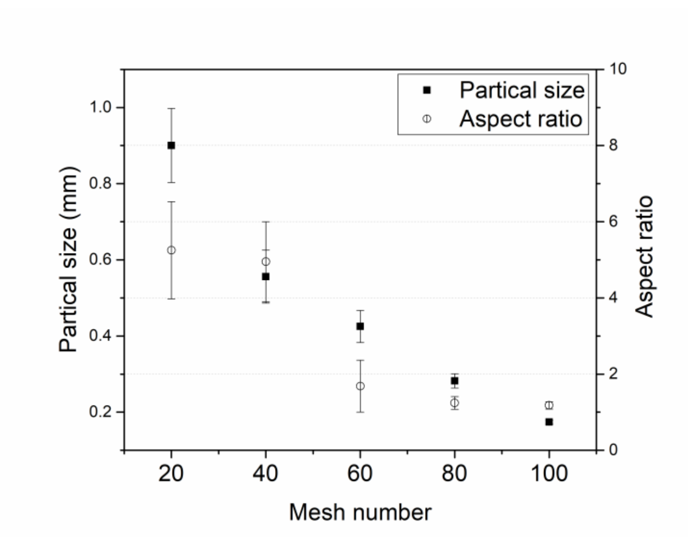

Figure 1. Particle size and aspect ratios of straw powder after screening with different mesh numbers.

2.2. Steel

Steel (ASTM 1045), which is widely used in open friction pairs such as screws and racks and pinions, was selected as the friction pair material in this study. Its hardness is 53 HRC (HR-150A, KAIYAN). The contact surface was treated before the test, and the surface roughness (Ra) was treated to 0.4 μm ± 0.1 μm (TR200, JIMTEC). The friction pairs are set as a pin and a disk. The pin is a cuboid with dimensions 10 × 10 × 20 mm, and the diameter and thickness of the disc are 150 mm and 5 mm, respectively. The contact area is 100 mm^2.

2.3. Lubricant

Commercial heavy-duty industrial gear oil (Mobil L-CKD, 85W-140) and commercial PTFE grease (KM-T23), commonly used in agricultural machinery, were selected as additional lubricants for this study.

2.4. Experimental Method

A pin-on-disk friction tester shown in Figure 2 (designed according ASME 99-2005 standard) was employed for this study. The motor directly drives the steel plate to rotate, and the pin body is fixed and connected to the force sensor. The force sensor measures the lateral force generated in the friction process, namely the friction force (F). The normal force value is determined by the load on the upper fixed block. The pin is placed in the position where the force sensor acts effectively. The coefficient of friction is calculated as $f = F/W$, where f is the coefficient of friction, and W is the normal force. The sampling rate is 100Hz. The friction coefficient is directly converted into a number by Labview and stored in the computer. Since the friction coefficient of the stable period of each test is different, the average friction coefficient is obtained according to the friction coefficient of the stable period under each test condition.

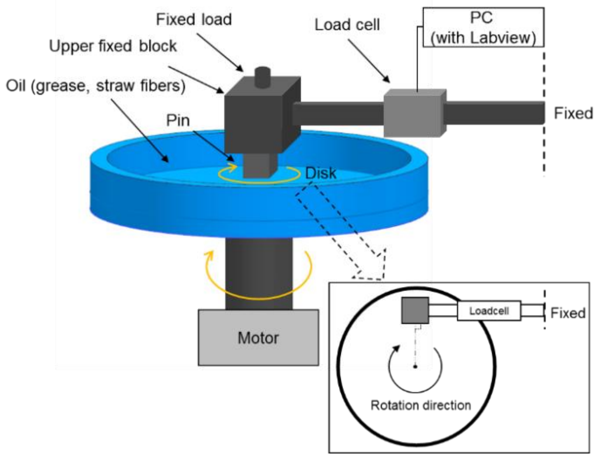

Figure 2. Pin-on-disk friction and wear tester.

Since the wear loss only accounts for a small part of the weight of the disc and the pin, the error is large if the wear rate is used to measure the wear performance. Therefore, the wear loss was used to explore the wear performance in this study, and the calculation formula is $\Delta M_{loss} = M_{(pin+disk)s} - M_{(pin+disk)f}$, where ΔM_{loss} is the wear loss, $M_{(pin+disk)s}$ is the total mass of the disk and pin before the test, and $M_{(pin+disk)f}$ is the total mass of the disk and pin after the test.

One gram of straw powder was naturally and evenly spread on the surface of the steel plate in a circular range with a diameter of 100 mm, and the thickness of the straw layer was 2 mm ± 0.6 mm. The pin was then pressed against the surface of the steel plate and the load was placed. As the test progressed, the centrifugal force of the rotation of the steel disk gradually threw the powder on the surface of the steel disk away from the contact surface. In order to match the actual working condition that the straw powder continues to enter the equipment, the powder was uniformly scattered into the rotation center at a speed of 2 g/min until the end of the test. For the test where we added lubricating oil, 1 g of straw powder was uniformly spread on the lubricated surface (10 mL) of the steel plate before the test start. According to the initial ratio of powder and oil, the lubricating oil was continuously added to the center of the pan at the rate of 20 mL of lubricating oil per 2 g of straw powder per minute, and the powder was sprinkled at the same time until the end of the test. Due to the high viscosity of PTFE grease, it does not detach from the surface with centrifugal force. Therefore, only the straw powder was added at a speed of 2 g/min until the end of the test for the test of PTFE grease mixed with straw powder.

Table 1 shows the experimental conditions. In order to ensure the reliability of the results, more than three tests were carried out for each condition. A new pin-on-disk sample was used for each test, and the parallelism of the pin-on-disk contact surface was corrected before each test. The experimental temperature and humidity were 28 °C ± 2 °C and 35% ± 4%, respectively. Regarding the operating pressure value of the open friction pair, 31.25 MPa was selected as the typical pressure value in this study.

Table 1. Experimental conditions.

Parameter, Unit	Value
Particle size, mm	0.17, 0.28, 0.43, 0.56, 0.90
Pressure, MPa	31.25
Linear velocity, m/s	0.1
Duration, min	40
Temperature, °C	28 ± 2 (Outdoor temperature in the summer)
Relative humidity, %	35 ± 4

3. Results and Discussion

3.1. Friction Property

Figure 3a shows the variation of the friction coefficient with time when the third body straw powder with different particle sizes is added under the condition of no lubricant. The friction coefficient initially increased rapidly, reached a peak after about 15 min, and then began to decrease slightly to a stable value. The friction transition period occurred before 15 min, followed by a stable period. The time-dependent trend of friction coefficient with the addition of 0.90 mm particle size powder was similar to that without the addition of powder. The friction coefficients with the addition of powder particle sizes of 0.17 mm–0.56 mm did not increase rapidly. When compared to the friction coefficient without powder, it can be seen that the friction coefficient with small particle size powder had no trend of rapid increase, indicating that the straw powder played a role in reducing the friction coefficient.

Under the condition of adding lubricant (Figure 3b,c), the friction coefficient without powder remained stable for the first 10 min and then rapidly increased to about 0.15. After reaching the maximum value around the 30th minute, it entered a stable period. The addition of lubricant delayed the rapid increase in the friction coefficient. After 10 min, the friction coefficient began to increase rapidly until it reached a stable value. The addition of 0.90 mm particle size straw powder showed similar results. When the small particle size powders were added, the friction coefficient still maintained a slow upward trend with time, and the increase was smaller than that of tests without lubricant. This also showed that the lubricant played a role in reducing wear.

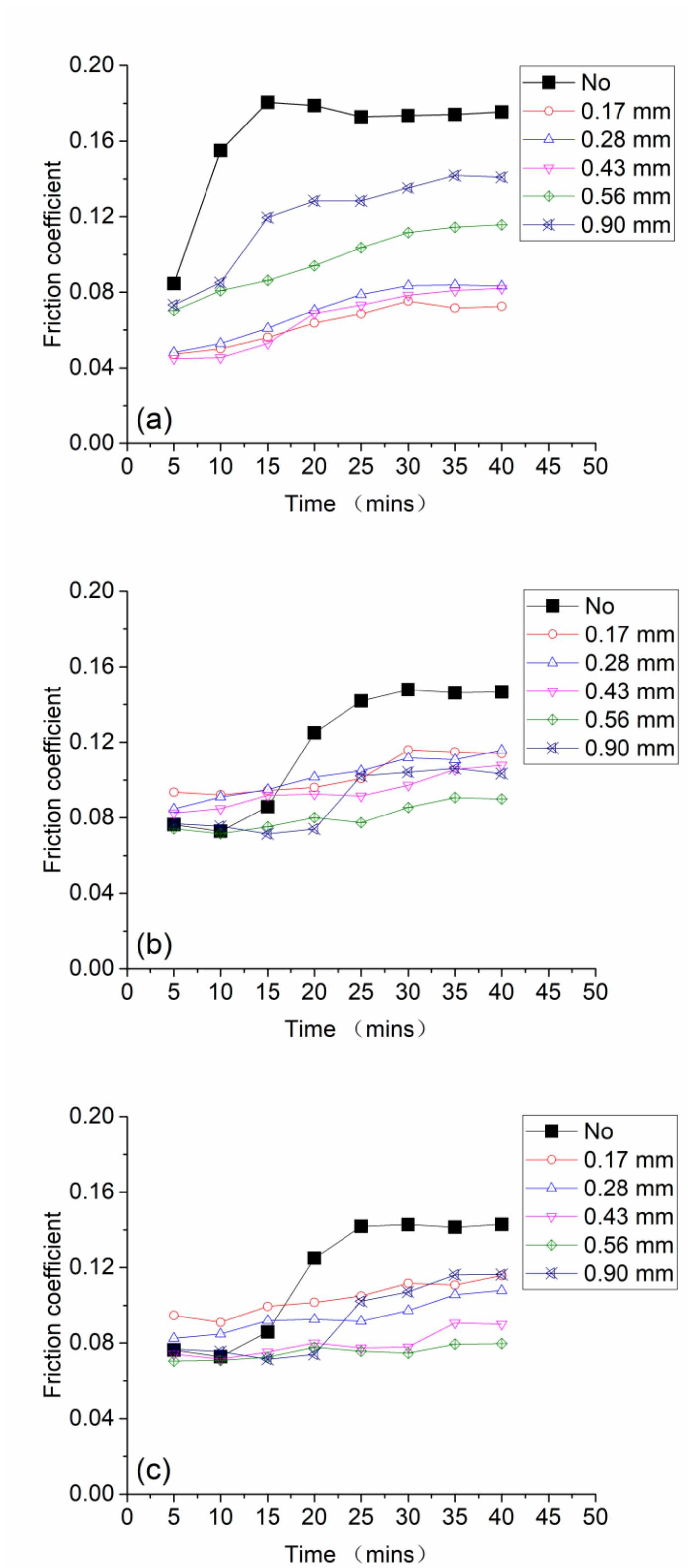

Figure 3. Variation curves of friction coefficient between steel–straw powder–steel with different particle sizes: (**a**) no lubricant; (**b**) lubricating oil; (**c**) lubricating grease

Figure 4 shows results of the average friction coefficient and standard deviation with powder of different particle sizes added. The friction coefficients with powder added were smaller than those without powder added under the same lubricating conditions, indicating that the straw powder played a role in reducing the friction coefficient. The straw powder acted as an isolation layer in the contact surface, which isolated the direct contact between the pin and the disc, reduced the contact area, and thus reduced the friction coefficient. This is also the reason for the decrease in the rising speed and amplitude of the friction coefficient in Figure 3.

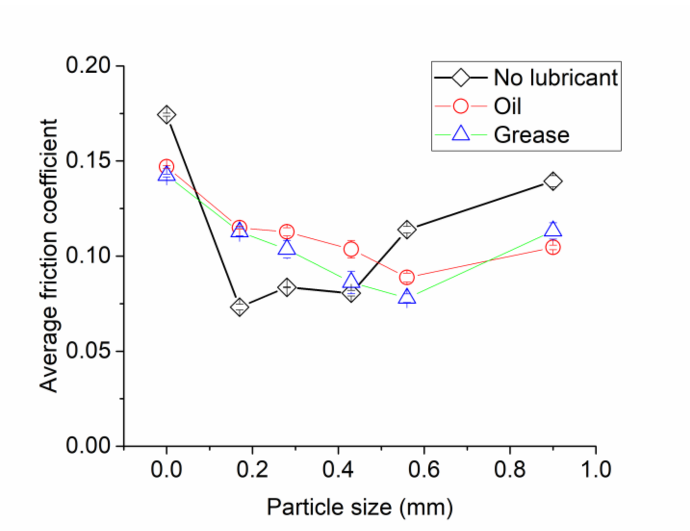

Figure 4. Average friction coefficient of straw powder with different particle sizes under various lubrication conditions.

When no lubricant was added, the average friction coefficient of the large particle size powders was greater than that of the small particle size powders. Although larger particle size powders were more effective at isolating direct pin and disc contact than smaller particle size powders, the results were the opposite. Combining Figure 4 with Figure 3a, it can be seen that the friction coefficient at the initial stage of friction was lower with large particle size straw powder than without straw powder, but then it increased rapidly. This might be due to the presence of straw powder in the interface before the start of the test, which played a certain role in isolation. However, as the friction progressed, the large particle size powder was gradually consumed. Moreover, due to the gradual reduction in the friction interface gap, the external large particle size powder could not continue to enter the friction interface (Figure 5) and could not play a continuous isolation effect, which resulted in the friction coefficient beginning to increase sharply around the 10th minute. However, the average particle size of straw powder within the contact surface reduced over time as shown in Figure 6. Due to the existence of finely ground powders in the friction interface or in the grooves caused by wear, some of the frictional stress is buffered, so that the friction coefficient is lower than that without powder addition.

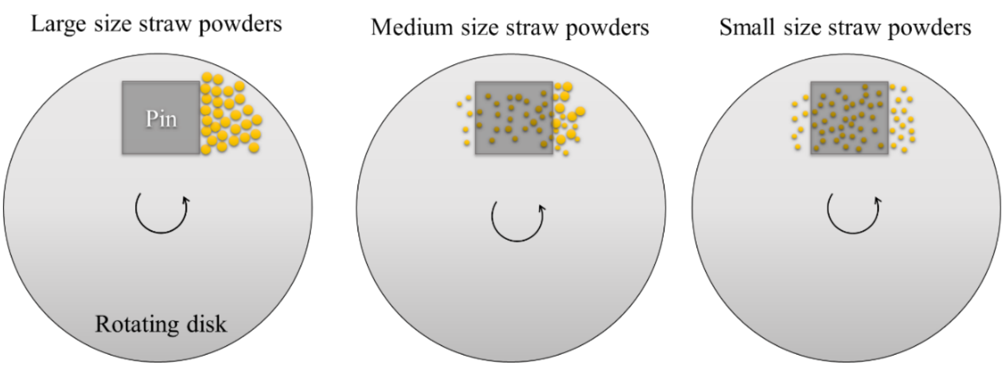

Figure 5. Movement of straw powder with different particle sizes during friction.

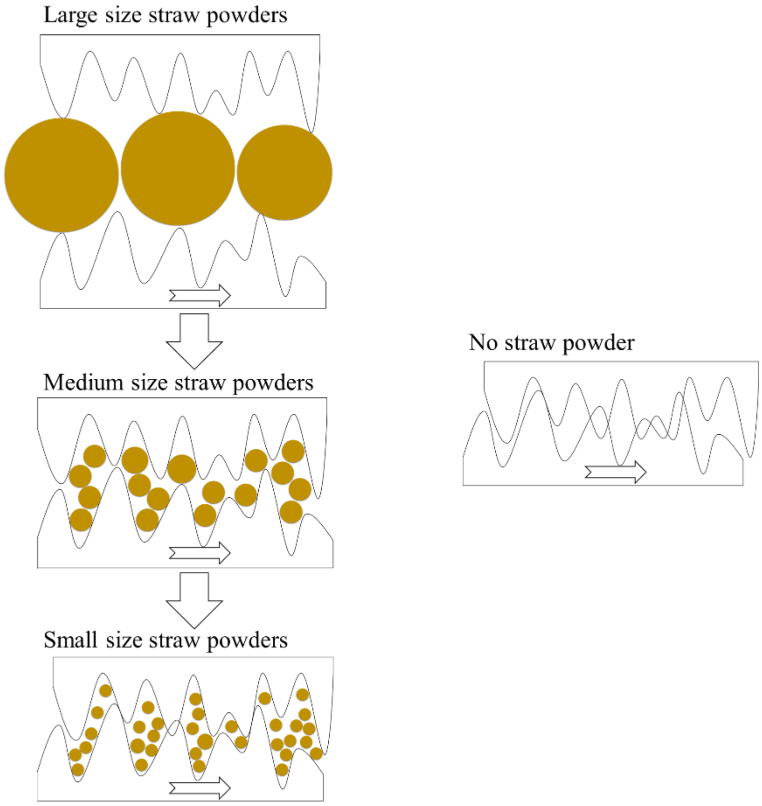

Figure 6. Behavior and evolution process of straw powders with different particle sizes at the contact interface.

When the lubricant was added, the friction coefficient decreased gradually with the increase in powder particle size. Under the coating of the lubricant, the large particle size powder was more likely to enter the friction interface, and the large particle size powder had a better isolation effect due to its large diameter, thereby reducing the friction coefficient. However, the powder with too large particle size (0.90 mm) could not continuously enter the contact interface, so it had no significant effect on the friction coefficient. Another possibility is that the straw powder has water and oil absorption. The oversized straw powder entering the friction interface was mixed with lubricating oil or grease and absorbed lubricant during the friction process, which resulted in volume expansion. In this case, the lubricating layer formed by the lubricant may also be destroyed, thereby leading to an increase in the friction coefficient. In addition, the friction coefficient of small particle size powder with the lubricant was greater than that without lubricant. The small particle size straw powder was pulled away from the surface micro-recesses because of the flow of added lubricant during the friction process, thereby destroying the original straw powder friction reduction system at the interface and increasing the friction coefficient.

3.2. Wear Property

Figure 7 shows the wear loss and standard deviation with various particle size powder under different lubrication conditions. When adding the same particle size powder, the wear with lubricant was smaller than that without lubricant, indicating that the lubricant also had a significant lubricating effect in the presence of straw powder.

Among the tests without lubricant, the wear was highest without straw powder. Adding straw powder significantly reduced the wear by about 50–60%. The addition of straw powder prevented direct contact between steel and steel and the straw powder particles embedded in the micro-recesses of the contact surface. This may also have buffered part of the friction stress, thereby reducing the wear. The wear with large particle size straw powder was larger than that with small particle size powder, because the large particle size powder could not continuously enter the friction interface. Moreover, the metal particles generated by the surface wear extruded the straw powder inside the dimples, which reduced the buffering effect of the straw powder on the frictional stress and increased the wear.

Regarding the results of the tests where lubricant was added, the wear without straw powder was the largest. Different from the results without the addition of lubricant, the particle size had no significant effect on the wear. Under the coating of the lubricant, the powder was integrated with the lubricant, and the lubricant as the matrix played a major role in the wear behavior.

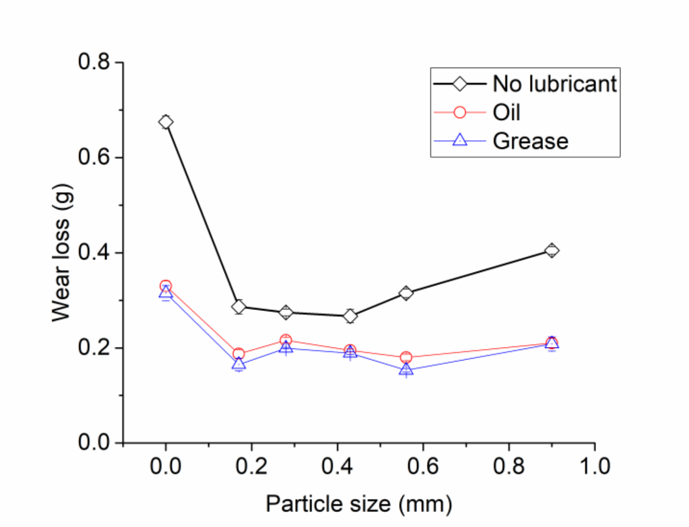

Figure 7. Average wear loss of straw powder with different particle sizes under various lubrication conditions.

Figure 8 shows the photomicrograph of a worn surface without lubricant. To ensure the scientificity of the results, the observed wear locations were randomly selected. Figure 8a–f are arranged beginning with no powder and continuing in ascending order of particle size. The worn surface without the straw powder showed obvious elongated deep grooves (furrows) and a small number of circular grooves. With the addition of straw powder, the furrows decreased significantly, but the micropores increased. When the particle size of the added powder was 0.56 mm and 0.90 mm, the furrows reappeared again.

When the pin and disc were in direct contact without any additional matter, there were obvious furrows and circular grooves, indicating that adhesion and abrasive wear occurred at the interface. The addition of straw powder significantly reduced the appearance of furrows. The circular grooves may be caused by the re-entry of the metal powder generated by the friction pair into the contact interface, causing wear on the surface. It could be speculated that the wear mechanism after straw powder addition changed from adhesive and abrasive mixed wear to abrasive wear. However, furrows reappeared when large particle size (0.56 mm and 0.90 mm) straw powder was added.

At the beginning of the test, there was initial straw powder between the contact interfaces. With the progress of the test, the large particle size straw powder that initially existed on the contact interface was slowly worn away and turned into smaller particle size powder. This small particle size powder still played a role as a friction isolation layer (Figure 6). When the surface was worn, the small particle size powder entered the micropores on the worn surface and quickly adhered and filled up the micropores. This reduced the frictional stress at the micro contact points and relieved the plastic deformation and wear of the contact surface, thereby reduced the shedding of abrasive particles and wear. However, as the particle size of the powder at the friction interface gradually became smaller, the gap of the friction pair gradually became smaller. Therefore, the large particle size powder could not continue to enter the interface and play a role in isolation (Figure 7), resulting in serious wear on the surface state. This was also the reason why the wear increased when the large particle size powder was added. Similar micropores were found on the worn surfaces of all samples where straw powder was added. These micropores showed a dull, non-reflective black in the photomicrograph, indicating that the interior of the micropores was likely non-reflective straw powder. This also indirectly explained that straw powder existed in the micropores, which buffered the frictional stress and reduced the friction coefficient and wear.

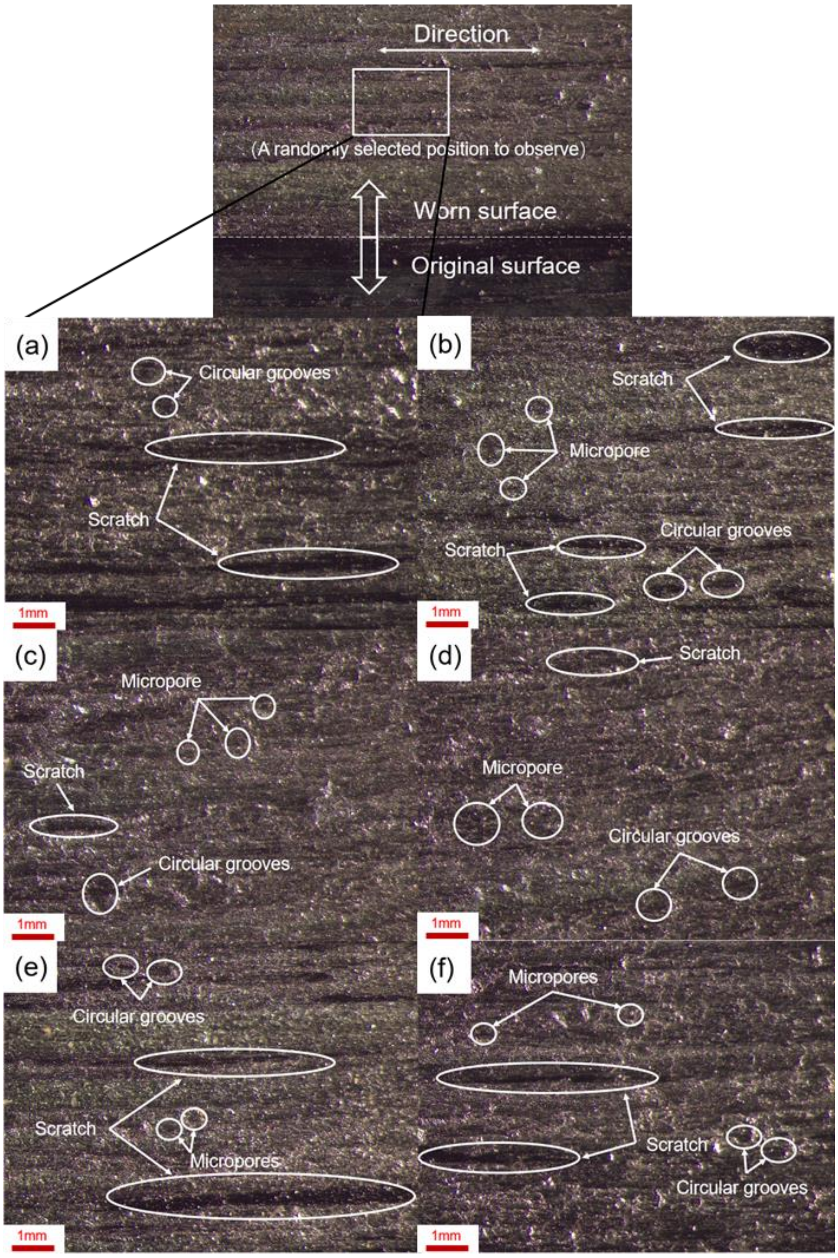

Figure 8. Worn disk surfaces with various particle sizes under no lubricant condition: (**a**) no powder added; (**b**) 0.17 mm; (**c**) 0.28 mm; (**d**) 0.43 mm; (**e**) 0.56 mm; (**f**) 0.90 mm.

Figure 9a–f show the photomicrographs of worn surfaces under lubrication oil conditions. Compared with the worn surfaces when lubricant was not added, the ploughing phenomenon of the worn surfaces when lubricating oil was added was significantly reduced, indicating that the lubricating oil had a significant lubricating effect. Moreover, almost no furrows were found on all worn surfaces when straw powder was added. In addition, there were obvious circular grooves on the worn surface, indicating that the friction behavior was dominated by abrasive wear when lubricating oil and straw powder were both added. Moreover, micropores were full of worn surfaces. The presence of straw powder in the micropores may also reduce the concentration of frictional stress on the surface, which played an auxiliary role in reducing the shedding of abrasive particles and wear. The particle size of the straw powder showed little effect on the worn surface when lubricating oil was added. Under the combined influence of lubricating oil and straw powder, the effect of lubricating oil is dominant.

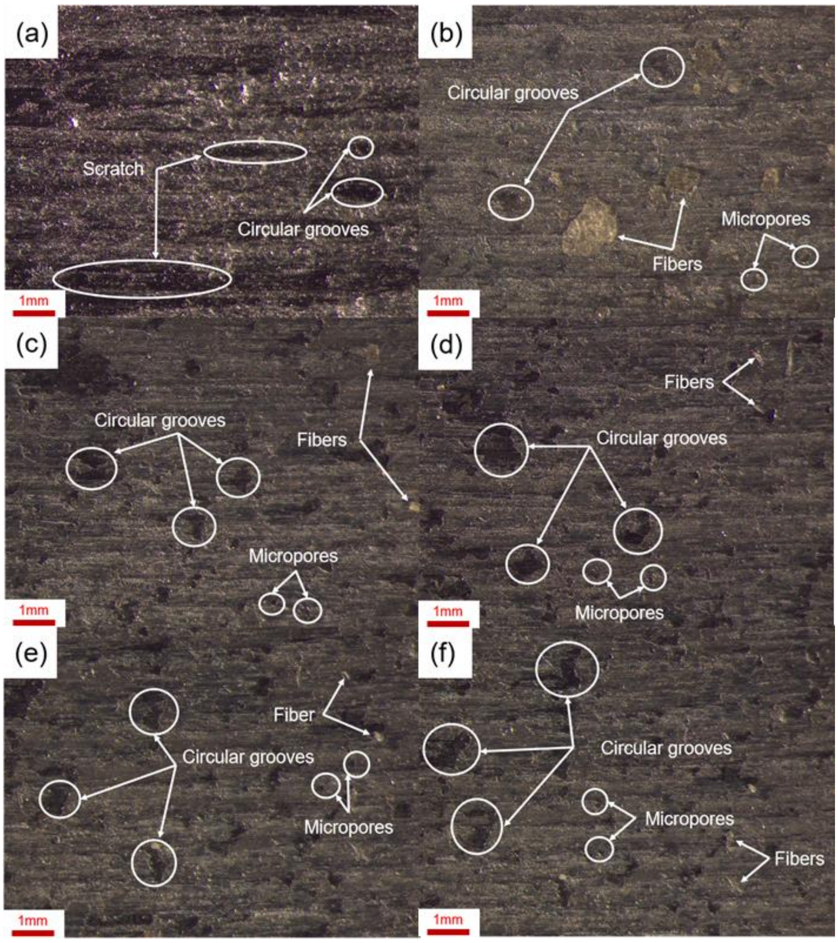

Figure 9. Worn disk surfaces with various particle sizes under lubricating oil condition: (**a**) no powder added; (**b**) 0.17 mm; (**c**) 0.28 mm; (**d**) 0.43 mm; (**e**) 0.56 mm; (**f**) 0.90 mm.

Figure 10a–f show the photomicrographs of worn surfaces under lubricating grease (PTFE grease) conditions. Results show that the surface wear was similar to that under lubricating oil conditions. Although there was a certain furrow phenomenon in the case where no straw powder was added, the degree was less than that without any lubricant added. The results also confirmed the high wear-reducing properties of PTFE grease. Under the condition of adding straw powder, the furrow phenomenon almost disappeared and was replaced by the appearance of circular grooves and micropores, indicating that the wear mechanism changed from adhesive and abrasive mixed wear to abrasive wear. Similar to the results when lubricating oil was added, the addition or lack of straw powder had no obvious effect on the wear under the lubricating grease condition. Since the straw powder was coated in grease, its influence was diminished, and the dominant influence was still PTFE grease.

For the third body friction properties of metal particles with high elastic modulus, whether the particle material is the same as the friction pair material is an important factor. As the friction temperature increases, the particles begin to soften, and the particles that are the same as the material of the friction pair begin to adhere to the friction pair, resulting in an increase in the friction coefficient [10]. Particles of different materials may form a smooth and dense oxide film between the contact interfaces, helping to reduce the coefficient of friction [11,12]. Because the straw powders did not stick to the metal significantly, a lubricating film was formed between the interfaces to reduce the friction coefficient. This paper only focuses on the friction experiments of wheat straw powder in crops. To confirm the third body friction properties of straw powder with different mechanical properties, further research is needed.

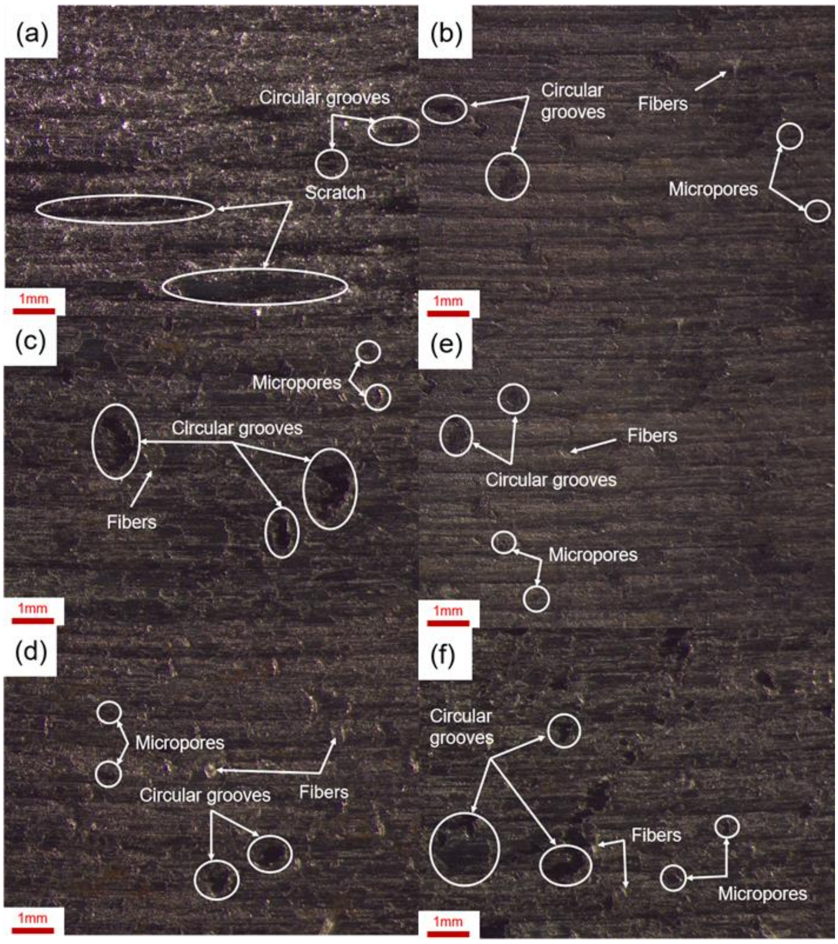

Figure 10. Worn disk surfaces with various particle sizes under lubricating grease condition: (**a**) no powder added; (**b**) 0.17 mm; (**c**) 0.28 mm; (**d**) 0.43 mm; (**e**) 0.56 mm; (**f**) 0.90 mm.

4. Conclusions

In this study, the pin-on-disk friction tester was employed to investigate the mechanism of third exogenous straw powder with different particle sizes on the friction and wear properties of the steel–steel friction pair. The results show that the addition of lubricating oil and lubricating grease significantly reduce the friction coefficient and wear. Further, different particle sizes of straw powder have an influence on the friction and wear properties of steel–steel friction pairs under various lubrication conditions. In general, straw powder with appropriate particle size (0.17 mm–0.56 mm) exists in the friction pair, which can play a certain role in reducing friction. Compared with straw powder with small particle size, that with large particle size is more likely to cause wear of the friction pair. Due to the limitation of laboratory conditions, it is difficult to simulate the actual friction process of straw powder in mechanical parts. Therefore, the results of this study can only provide a reference for the third body friction and wear performance of straw powder and the design of friction pairs.

Author Contributions: Conceptualization, C.L.; methodology and software, C.L. and W.Z.; formal analysis, C.L. and X.D.; investigation, W.Z.; resources, Y.L.; data curation, C.L.; writing—original draft preparation, C.L.; writing—review and editing, S.W. and P.Z. All authors have read and agreed to the published version of the manuscript.

Funding: This research was funded by the Project of Shandong Provincial Natural Science Foundation, grant number ZR2021MC095; the Project of Shandong Provincial Agricultural Science and Technology Foundation (Forestry Science and Technology), grant number 2019LY008; Science and Technology Support Program for Youth Innovation Team in Colleges and Universities of Shandong Province, China, grant number 2020KJF012; Key Laboratory of Bio-based Material Science & Technology , Ministry of Education, grant number SWZ-MS201912; and Jiangsu Provincial Policy Guidance Program (Special Project of Science and Technology for Northern Jiangsu), grant number SZ-SQ2020031.

Institutional Review Board Statement: Not applicable.

Informed Consent Statement: Not applicable.

Data Availability Statement: Not applicable.

Conflicts of Interest: The authors declare no conflicts of interest.

References

1. Bhushan, B. *Introduction to Tribology*; John Wiley & Sons: Hoboken, NJ, USA, 2013.
2. Singer, I.L. How Third-Body Processes Affect Friction and Wear. *MRS Bulletin*. **1998**, *23*, 37–40.
3. Deng, F.; Tsekenis, G.; Rubinstein, S.M. Simple Law for Third-Body Friction. *Phys. Rev. Lett.* **2019**, *122*, 135503.
4. Qin, K.; Zhou, Q.; Zhang, K.; Feng, Y.L.; Zhang, T.; Zheng, G.J.; Xia, B.R.; Liu, B.L. Non-uniform abrasive particle size effects on friction characteristics of FKM O-ring seals under three-body abrasion. *Tribol. Int.* **2019**, *136*, 216–223.
5. Gheisari, R.; Polycarpou, A.A. Three-body abrasive wear of hard coatings: Effects of hardness and roughness. *Thin Solid Films* **2018**, *666*, 66–75.
6. Wu, H.W.; Chen, Y.Y. Effect of two-body and three-body microcontacts under dry friction on contact characteristics. *Proc. Inst. Mech. Eng. Part C J. Eng. Mech. Eng. Sci*. **2018**, *232*, 706–719.
7. Wu, H.W.; Chen, Y.Y.; Horng, J.H. The Analysis of Three-Body Contact Temperature under the Different Third Particle Size, Density, and Value of Friction. *Micromachines* **2017**, *8*, 302.
8. Wu, H.W.; Chen, Y.Y.; Horng, J.H. Contact temperature under three-body dry friction conditions. *Wear* **2015**, *330*, 85–92.
9. Woldman, M.; Van der Heide, E.; Tinga, T.; Masen, M.A. The influence of abrasive body dimensions on single asperity wear. *Wear* **2013**, *301*, 76–81.
10. Su, L.; Gao, F.; Han, X.; Chen, J. Effect of copper powder third body on tribological property of copper-based friction materials. *Tribol. Int.* **2015**, *90*, 420–425.
11. Su, L.L.; Gao, F.; Han, X.M.; Fu, R.; Zhang, E. Tribological Behavior of Copper-Graphite Powder Third Body on Copper-Based Friction Materials. *Tribol. Lett*. **2015**, *60*, 12.
12. Su, L.L.; Gao, F.; Wang, L.X.; Han, X.M.; Fu, R.; Tao, H.L. Iron Powder Third Body Contribution to Friction Performance of Copper-Matrix Friction Composites. *Tribol. Trans*. **2019**, *62*, 486–495.
13. Gheisari, R.; Polycarpou, A.A. Tribological performance of graphite-filled polyimide and PTFE composites in oil-lubricated three-body abrasive conditions. *Wear* **2019**, *436*, 11.
14. Qin, K.; Zhou, Q.; Zhang, K.; Lv, M. Effect of Thermal Degradation of FKM on Three-Body Abrasion under Dry Sliding: Severe Damage Led by the Particle Detention. *Materials* **2021**, *14*, 3820.
15. Diomidis, N.; Mischler, S. Third body effects on friction and wear during fretting of steel contacts. *Tribol. Int.* **2011**, *44*, 1452–1460.
16. Du, X.Y.; Yang, J.Y.; Gao, F.; Han, X.M.; Su, L.L. Mechanisms of the copper third body as an interfacial media on copper matrix friction materials with different compositions. *Ind. Lubr. Tribol*. **2021**, *73*, 1011–1018.
17. Miftakhova, A.; Chen, Y.Y.; Horng, J.H. Effect of rolling on the friction coefficient in three-body contact. *Adv. Mech. Eng.* **2019**, *11*, 9.
18. Ardila, M.A.N.; Costa, H.L.; de Mello, J.D.B. Influence of the ball material on friction and wear in microabrasion tests. *Wear* **2020**, *450*, 11.
19. Mattetti, M.; Molari, G.; Sereni, E. Damage evaluation of driving events for agricultural tractors. *Comput. Electron. Agric*. **2017**, *135*, 328–337.

20. Cucinotta, F.; Scappaticci, L.; Sfravara, F.; Morelli, F.; Mariani, F.; Varani, M.; Mattetti, M. On the morphology of the abrasive wear on ploughshares by means of 3D scanning. *Biosyst. Eng.* **2019**, *179*, 117–125.
21. Mironov, D.; Sidorov, S.; Liskin, I. Strength and Durability Characteristics of Soil-Cutting Working Tools. *Agric. Mach. Technol.* **2019**, *13*, 39–43.
22. Scolaro, E.; Beligoj, M.; Estevez, M.P.; Alberti, L.; Renzi, M.; Mattetti, M. Electrification of Agricultural Machinery: A Review. *IEEE Access* **2021**, *9*, 164520–164541.
23. Li, D.; Zheng, Y.; Zhao, W. Fault Analysis System for Agricultural Machinery Based on Big Data. *IEEE Access* **2019**, *7*, 99136–99151.
24. Cao, R.Y.; Li, S.C.; Ji, Y.H.; Zhang, Z.Q.; Xu, H.Z.; Zhang, M.; Li, M.Z.; Li, H. Task assignment of multiple agricultural machinery cooperation based on improved ant colony algorithm. *Comput Electron Agric*. **2021**, *182*, 8.